JNeurosci
THE JOURNAL OF NEUROSCIENCE

Research Articles | Systems/Circuits

AgRP neurons as an integrative node linking the somatotropic and reproductive axes

https://doi.org/10.1523/JNEUROSCI.1013-26.2026

Received: 16 June 2026
Revised: 6 October 2026
Accepted: 30 October 2026

Copyright © 2026 the authors

This Early Release article has been peer reviewed and accepted, but has not been through the composition and copyediting processes.The final version may differ slightly in style or formatting and will contain links to any extended data.

Alerts: Sign up at www.jneurosci.org/alerts to receive customized email alerts when the fully formatted version of this article is published.

AgRP neurons as an integrative node linking the somatotropic and reproductive axes

Guilherme Andrade Alves[1], Henrique Rodrigues Vieira[1], Ligia M M de Sousa[2], Edward O. List[3], John J. Kopchick[3], Luiz Mauricio Valentin Sousa[4], Juneo Freitas Silva[4], Jose Donato Jr[2], *Renata Frazao[1]

[1] Universidade de Sao Paulo, Instituto de Ciencias Biomedicas, Departamento de Anatomia, Sao Paulo, Brazil

[2] Universidade de Sao Paulo, Instituto de Ciencias Biomedicas, Departamento de Fisiologia e Biofísica, Sao Paulo, Brazil

[3] Institute of Molecular Medicine and Aging, Ohio University, Heritage College of Osteopathic Medicine, Athens, Ohio, USA

[4] Universidade Estadual de Santa Cruz, Centro de Microscopia Eletronica, Departamento de Ciencias Biologicas, Bahia, Brazil

* Corresponding author

Renata Frazao, Ph.D.

https://orcid.org/0000-0002-0877-8453

Address: Av. Prof. Lineu Prestes, 2415, São Paulo, Brazil, 05508-000

Email: rfrazao@usp.br

Phone: +55-11-3091-0932; Fax: +55-11-3091-7366

DISCLOSURE SUMMARY:

Number of pages: 32

Number of figures: 5

Number of tables: 4

Number of words for Abstract: 231

Number of words for Significance Statement: 100

Number of words for Introduction: 626

Number of words for Discussion: 1496

Conflict of interest

The authors declare no competing financial interests.

JNeurosci Accepted Manuscript

Author contributions: R.F designed research; G.A.A, H.R.V, L. M. M. S, performed research; E.O.L., J.J.K., J.F.S. contributed unpublished reagents/analytic tools; G.A.A, R.F, L.M.V.S, J.F.S. analyzed data; H.R.V, L.M.M.S, E.O.L., J.J.K., J.F.S, J.D.J. edited the paper; G.A.A, and R.F. wrote the paper

Acknowledgments: This study was supported by the São Paulo Research Foundation [FAPESP grant numbers: 2021/08792-0 (GAA); 2023/11833-5 (LMMS), 2024/21641-9 (JDJ), 2022/11262-5 and 2025/22689-8 (RF)], the Coordenação de Aperfeiçoamento de Pessoal de Nível Superior (CAPES) - Finance Code 001" (HRV), and by the Conselho Nacional de Desenvolvimento Cientifico e Tecnologico (CNPq; JDJ, JFS, and RF).

JNeurosci Accepted Manuscript

Abstract

Growth hormone (GH) signaling contributes to pubertal development and reproductive function, yet the hypothalamic circuits mediating these effects remain incompletely understood. Kisspeptin and agouti-related protein (AgRP) neurons are key integrators of metabolic and reproductive cues and exhibit GH-responsive signaling pathways. We therefore investigated their contributions to the reproductive consequences of altered somatotropic signaling. Using genetic mouse models of chronic GH excess or deficiency, we examined the impact of altered GH signaling on pubertal maturation, fertility, and hypothalamic neuroendocrine function. Pubertal onset was unaffected in female mice, whereas males with either GH excess or GH deficiency exhibited delayed puberty. In contrast, GH hypersecretion selectively disrupted estrous cyclicity and impaired fertility in females. Female reproductive dysfunction occurred despite preserved kisspeptin signaling, as evidenced by the preservation of intrinsic electrophysiological properties of kisspeptin neurons and unaltered hypothalamic *Kiss1* mRNA expression. Chronic GH excess increased hypothalamic *Agrp* mRNA expression and reduced *Pomc* and *Tac2* mRNA expression compared to control mice; these transcriptional changes were prevented by AgRP-specific GH receptor (GHR) deletion, which also improved ovarian function. Notably, selective deletion of the GHR in AgRP cells markedly improved fertility in GH-hypersecreting females. Together, these findings identify AgRP neurons as a critical hypothalamic target through which chronic GH excess impairs female reproductive function. Our results further demonstrate that GH-induced infertility occurs independently of canonical kisspeptin-GnRH dysfunction, revealing a sexually dimorphic mechanism linking somatotropic signaling to reproductive competence.

Keywords: Fertility; Growth hormone; Hypothalamus; Kisspeptin; Puberty; Sexual dimorphism.

JNeurosci Accepted Manuscript

Significance Statement

Reproductive dysfunction is a common consequence of chronic alterations in growth hormone (GH) secretion, but the underlying neural mechanisms remain poorly defined. We show that chronic GH excess induces a sexually dimorphic reproductive phenotype characterized by profound impairment of female fertility despite largely preserved kisspeptin neuronal function. In contrast, GH excess altered hypothalamic AgRP-associated pathways, and the selective deletion of GH receptors in AgRP neurons significantly improved fertility in GH-hypersecreting females. These findings identify AgRP neurons as key mediators of GH-induced reproductive dysfunction and reveal a previously unrecognized sexually dimorphic neuroendocrine mechanism linking somatotropic signaling, metabolic circuits, and female fertility.

JNeurosci Accepted Manuscript

Introduction

Growth hormone (GH) and its principal downstream effector, insulin-like growth factor 1 (IGF-1), are key regulators of somatic growth and metabolism (Ranke and Wit, 2018; Donato et al., 2021; de Sousa et al., 2025). GH secretion is controlled by a complex neuroendocrine system involving hypothalamic GH-releasing hormone and somatostatin, circulating ghrelin, and IGF-1, which together regulate GH secretion through stimulatory and inhibitory feedback mechanisms at hypothalamic and pituitary levels (Steyn et al., 2016; de Sousa et al., 2025). In addition to their classical actions, substantial evidence indicates that alterations in somatotropic signaling influence pubertal timing and fertility. GH deficiency or resistance is associated with delayed sexual maturation and impaired reproductive capacity, whereas chronic GH excess disrupts reproductive function and shortens reproductive lifespan in males and females (Advis et al., 1981; Savage et al., 1993; Cecim et al., 1995a; de Boer et al., 1997; Bartke, 1999; Danilovich et al., 1999; Keene et al., 2002; Zaczek et al., 2002; Smuel et al., 2015; de Paula et al., 2021). Despite these observations, the neural mechanisms through which the somatotropic axis modulates reproductive physiology remain poorly understood.

Reproduction is tightly coupled to metabolic state, and hypothalamic circuits are central to this integration (Anderson et al., 2024). Among the principal regulators of reproduction are *Kiss1*-expressing neurons (hereafter referred to as kisspeptin neurons), which are essential for pubertal maturation and fertility (Lehman et al., 2018). Kisspeptin neurons are responsive to GH, ghrelin, and IGF-1 signaling, suggesting that the somatotrophic axis may influence reproductive function through direct actions on these neurons (Frazao et al., 2014; Bohlen et al., 2019; Silveira et al., 2019; Silva et al., 2026). Kisspeptin neurons are also extensively interconnected with hypothalamic circuits controlling energy homeostasis, including agouti-related peptide (AgRP) neurons (Backholer et al., 2010; Donato et al., 2011; Steyn et al., 2013; Manfredi-Lozano et al., 2016; Nestor et al., 2016; Padilla et al., 2017; Qiu et al., 2018; Ross et al., 2018; Merkley et

JNeurosci Accepted Manuscript

al., 2021; Stincic et al., 2021; Mansano et al., 2023; Talbi et al., 2025). These neuroanatomical and functional connectivity data suggest that metabolically oriented hypothalamic pathways contribute to the reproductive alterations associated with chronic somatotropic dysregulation.

Within the arcuate nucleus of the hypothalamus (ARH), AgRP neurons are activated during negative energy balance and promote food seeking while suppressing energetically costly processes, including reproduction (Krashes et al., 2011). Growing evidence indicates that AgRP neurons function as gatekeepers of reproductive competence, as their activation suppresses gonadotropin secretion, disrupts estrous cyclicity, and impairs fertility (Padilla et al., 2017; Coutinho et al., 2020). Moreover, AgRP neurons are direct targets of GH and IGF-1 signaling (Furigo et al., 2019; Farias Quipildor et al., 2021). Intraperitoneal GH administration induces phosphorylation of signal transducer and activator of transcription 5 (STAT5) in approximately 90% of AgRP neurons, indicating widespread GH responsiveness within this neuronal population (Furigo et al., 2019). GH also increases hypothalamic *AgRP* and neuropeptide Y (*Npy*) mRNA expression and depolarizes AgRP neurons (Furigo et al., 2019), suggesting these neurons may provide a cellular substrate linking the somatotropic state to reproductive competence. However, whether chronic alterations in GH signaling engage AgRP circuits to regulate fertility remains unknown. More broadly, the relative contribution of primary reproductive circuits, such as kisspeptin neurons, versus metabolically oriented hypothalamic pathways in mediating the reproductive consequences of chronic GH imbalance remains unresolved.

Here, we tested the hypothesis that chronic somatotropic dysregulation alters reproductive function through hypothalamic circuits that integrate metabolism and fertility. Using mouse models of GH excess and GH deficiency, we first examined sex-specific effects on pubertal timing and fertility. We then focused on females with chronic GH excess to define the neural and endocrine mechanisms underlying subfertility. These studies

JNeurosci Accepted Manuscript

identify hypothalamic mechanisms through which chronic somatotropic imbalance disrupts female reproductive function.

JNeurosci Accepted Manuscript

MATERIALS AND METHODS

Animals

Kiss1-hrGFP mice (stock nº: 023425, The Jackson Laboratory, Bar Harbor, ME, USA) were bred with bGH transgenic mice (Berryman et al., 2004) to obtain the Kiss1-hrGFP/bGH animals (hereafter referred to as bGH). The GH transgenic model, generated on a C57BL/6J background, carries the bovine growth hormone (bGH) transgene under the control of the metallothionein promoter, resulting in constitutive GH overexpression and chronically elevated GH signaling (Berryman et al., 2004). Ghrhr^{lit} animals (stock nº: 000533, The Jackson Laboratory) were used as a model of spontaneous GH deficiency. This model carries a spontaneous mutation in the growth hormone-releasing hormone receptor (*Ghrhr*) gene on the C57BL/6J background, and homozygous Ghrhr$^{lit/lit}$ animals exhibit impaired pituitary GH secretion. Homozygous Ghrhr$^{lit/lit}$ animals were generated by breeding heterozygous mice within the colony. Selective ablation of GHR in AgRP cells was achieved by breeding AgRP-Cre mice (stock nº: 012899, The Jackson Laboratory) with GHR$^{flox/flox}$ animals (List et al., 2013; List et al., 2014) and bGH animals to obtain the AgRP-Cre/GHR$^{flox/flox}$/bGH mice (AgRP GHR KO/bGH). Control mice were AgRP-Cre/GHR$^{flox/flox}$ littermates lacking the bGH transgene (AgRP GHR KO).

Animals were weaned at three weeks of age and genotyped using polymerase chain reaction (PCR). Genomic DNA was obtained from tail tips using the REDExtract-N-Amp Tissue PCR Kit (Sigma, St. Louis, MO, USA). Animals were housed in environmentally controlled rooms in groups of 4 to 5 per cage. They were maintained on a 12-hour light/dark cycle (lights on at 06:00 AM) at 21-23°C. The Animal Ethics Committee of the Institute of Biomedical Sciences at the University of Sao Paulo approved all procedures.

Sexual maturation, estrous cycle, and fertility evaluation

We assessed sexual maturation by recording the ages at vaginal opening and the first day of estrus in female mice, and measuring the ages at testicular descent and balano-

JNeurosci Accepted Manuscript

preputial separation in male mice, as previously described (Bohlen et al., 2016; de Paula et al., 2021). Body weight was recorded on the specific days when sexual maturation events were observed. We evaluated estrous cycles in adult mice by collecting vaginal lavage samples daily for 30 days from 8 to 12 weeks of age. Specific cell types characteristic of each phase of the estrous cycle was identified (Gusmao et al., 2022). In addition, adult males and females (12-18 weeks of age) were mated with age-matched and sexually experienced female and male control mice to assess fertility. Matings were monitored for 60 days. The fertility rate was determined using pregnancy detection, the number of days to delivery (latency to delivery), and the number of pups per litter, as previously described (Silveira et al., 2017).

Hormone assessment

For LH and FSH measurement, we handled mice for 30 days to habituate them to the tail-tip blood sampling procedure (Steyn et al., 2013). Whole blood was collected from the tail tip before the end of the light cycle (5 ml). We collected a single blood sample to determine LH and FSH levels on the first day of diestrus. Serum LH and FSH levels were determined using an in-house sensitive sandwich enzyme-linked immunosorbent assay (ELISA) (Steyn et al., 2013). The LH and FSH ELISA have lower limits of detection of 0.009 ng/mL and 0.34 ng/mL, respectively, considering the dilution factors used (5x for LH and 10x for FSH).

For IGF-1 or testosterone measurement, adult mice (8-12 weeks of age) or pubertal mice (28-30 days of age) were anesthetized with isoflurane, euthanized by decapitation, and the trunk blood was collected. We centrifuged the blood to obtain serum and stored it at −80°C until analysis. IGF-1 or testosterone concentrations were measured using commercially available ELISA (IGF-1, #MG100, R&D Systems; Testosterone, # TE187S-100, Calbiotech). The lower limit of detection for the IGF-1 assay was 0.0035 ng/mL, whereas the analytical sensitivity of the testosterone assay was 0.1 ng/mL. The intra-assay

JNeurosci Accepted Manuscript

and inter-assay coefficients of variation were 4.3% and 6.0% for the IGF-1 assay, and 6.4% and 9.7% for the testosterone assay, respectively.

Quantitative Real-Time PCR

The total hypothalamus of adult female (diestrus) and male mice (21-25 weeks of age) was collected (10:00 a.m. - 12:00 p.m.). Total RNA was extracted from the hypothalamus using TRIzol reagent according to the manufacturer's instructions (Thermo Fisher Scientific, Waltham, USA). As previously described (Bohlen et al., 2019), extracted RNA was quantified and subsequently subjected to a pre-treatment step in which 3.36µl of $MgCl_2$ (Roche Applied Science), 0.32µl of DNase, and a specific volume of DEPC-treated water were added to each sample to reach a final volume of 20µl. Samples were incubated in a thermal cycler for 30 minutes at 37ºC, 10 minutes at 75ºC, and held for a few minutes at 4ºC. Complementary DNA (cDNA) was synthesized using the SuperScript II Reverse Transcriptase kit (Thermo Fisher Scientific). The reaction mix included 20µl of 5x buffer, 10µl of DTT, 20µl of dNTPs (10mM), 10µl of random primer (pdN_6) (Roche Applied Science), 20µl of DEPC-treated water, and 1µl of SuperScript II Reverse Transcriptase. Samples were incubated in a thermal cycler for 10 minutes at 25ºC, 50 minutes at 42ºC, 10 minutes at 72ºC, and held for a few minutes at 4ºC. The resulting cDNA samples were stored at -20ºC. Gene expression was quantified by real-time quantitative PCR using SYBR® Green enzyme (Thermo Fisher Scientific). For each reaction, 1.5 µl of cDNA was combined with 3.25 µl of DEPC-treated water, 1.5 µl of gene-specific primers (2.5 µM), and 6.25 µl of SYBR® Green master mix. All samples were run in duplicate, and negative controls were included on each plate. The following genes were analyzed: *Actb* (forward: gctccggcatgtgcaaag; reverse: catcacaccctggtgccta), *Agrp* (forward: ctttggcggaggtgctagat; reverse: aggactcgtgcagccttacac), *Gnrh1* (forward: gggttctgccatttgatccac; reverse: ccctttgactttcacatcc), *Kiss1* (forward: gattccttttcccaggcatt; reverse: ggcaaaagtgaagcctggat), *Npy* (forward: cagatactactccgctctgcg reverse: gggctggatctcttgccata), *Pdyn* (forward:

JNeurosci Accepted Manuscript

tgtgcagtgaggattcaggatg reverse: accgtcagggtgagaaaagatg), *Ppia* (forward: cttcttgctggtcttgccattcc reverse: tatctgcactgccaagactgagt), *Pomc* (forward: tagatgtgtggagctggtgc; reverse: ccagcgagaggtcgagtttg), *Esr1* (forward: gcagatagggagctggttca, reverse: tggagattcaagtccccaaa) and *Tac2* (forward: tgcatgtcacgtttctgtgg; reverse: ccgctccatctctctggaag). Plates containing the samples and target genes were analyzed using the 7500 Real-Time PCR System (Applied Biosystems), and relative mRNA quantification was performed using the $2^{-\Delta\Delta Ct}$ method.

Electrophysiological recordings

Adult bGH and control female mice (8-12 weeks of age, at diestrus) were selected for electrophysiological experiments. Following anesthesia (isoflurane 5%), animals were euthanized, and the brain was extracted. Each brain was sectioned into 250 µm-thick coronal slices in cutting solution (238 mM sucrose, 2.5 mM KCl, 26 mM $NaHCO_3$, 1 mM NaH_2PO_4, 10 mM D-glucose, 1 mM $CaCl_2$, and 5 mM $MgCl_2$) using a vibratome (Leica). The brain slices were maintained in carbogen-saturated (95% O2 and 5% CO2) containing 135 mM NaCl, 26 mM $NaHCO_3$, 1.25 mM NaH_2PO_4, 1.2 mM $MgSO_4$, 10 mM D-glucose, 3.5 mM KCl, and 1mM $CaCl_2$ for at least 1 hour before the start of electrophysiological recordings. Brain slices were transferred one at a time to a recording chamber mounted on a microscope. Slices were continuously perfused with oxygenated ACSF (30ºC) at a flow rate of ~2 ml/min. Resting membrane potential (RMP) was recorded in current-clamp mode (I=0). Neurons were identified by their endogenous expression of the fluorescent protein hrGFP using fluorescence microscopy (Leica MD 6000 FS microscope equipped with a fixed-stage platform and high-speed monochrome digital fluorescence camera, Leica DFC360). After identification, infrared differential interference contrast (IR-DIC) was used to establish a seal and achieve whole-cell access. The micropipette solution was composed of 130 mM K gluconate, 15 mM KCl, 10 mM HEPES, 5 mM EGTA, 0.1 mM $CaCl_2$, 4.0 mM MgATP, 0.4 mM NaGTP, and 8.5 mM NaOH, pH 7.3 (ECL = -56 mV). When filled, the

JNeurosci Accepted Manuscript

micropipettes had a resistance of 5–7 MΩ. The input resistance was assessed by measuring the voltage deflection at the end of the response to a hyperpolarizing rectangular current pulse (500 ms of −10 to −30 pA). The membrane potential values were corrected for the liquid junction potential (-15 mV).

For GABAergic spontaneous postsynaptic currents (sPSC) recordings, the recording pipette was filled with an isotonic chloride-based internal solution (140 mM KCl, 10 mM HEPES, 5 mM EGTA, 0.1 mM $CaCl_2$, 8.5 mM NaOH, 4 mM Mg-ATP, 0.4 mM Na-GTP; pH 7.3 (ECL = 0 mV)). When filled, the micropipettes had a resistance of 3-4.5 MΩ. During recordings, slices were perfused with ACSF containing 50 µM 6-cyano-7-nitroquinoxaline-2,3-dione (CNQX) and 50 µM 2-amino-5-phosphonovalerate (DLAP-5). Experiments were conducted in whole-cell configuration under voltage-clamp mode. Traces were recorded with the membrane potential held at -60 mV for 2 minutes.

The electrophysiological signals from kisspeptin neurons were recorded using an Axopatch 700B amplifier (Molecular Devices, San Jose, CA, USA; RRID:SCR_011323), low-pass filtered at 2 to 4 kHz, and analyzed offline on a PC with pCLAMP (Molecular Devices). GABAergic sPSC frequency and amplitude were analyzed with the Mini Analysis Program (Synaptosoft, Decatur, GA, USA; RRID:SCR_002184). For all recordings, series resistance was <20 MΩ, and data were discarded if a change of 20% or more occurred during the recording.

Ovarian Morphological Analysis

Adult animals (21-25 weeks of age) were anesthetized and euthanized. We collected tissues during the diestrus phase in the morning. We harvested and weighed the uterus. We rinsed ovaries in PBS and immediately immersed them in 10% formalin at room temperature for 48 hours. Samples were subjected to a standard histological processing protocol with increasing concentrations of ethanol and xylene, and then embedded in Paraplast®. Nine sections (4µm) per animal, with 40 µm spacing between them, were cut

JNeurosci Accepted Manuscript

using a Leica RM2145 microtome and subsequently stained with hematoxylin-eosin (H&E). Primary, secondary, antral, and atretic follicles, as well as degenerated retained oocytes and corpora lutea, were counted blindly by two independent examiners (Meng et al., 2017; de Oliveira et al., 2022). Degenerated retained oocytes were defined as terminal remnants of atretic follicles characterized by a morphologically degenerated oocyte with loss of normal follicular architecture, representing advanced follicular atresia (Inoue et al., 2000). Data were expressed as the number of structures per histological section.

Statistical analyses

Statistical analyses were performed using the GraphPad Prism software (GraphPad Prism; RRID: SCR_002798). The data were tabulated and presented as mean ± standard error of the mean. Data were checked for normality and homogeneity of variance using the Shapiro-Wilk and Kolmogorov-Smirnov tests. Parametric data were compared using an unpaired two-tailed Student's t-test. Non-parametric data were compared using the Mann–Whitney test. Fisher's exact test was used to assess fertility rates. For GH and IGF-1 concentrations, two separate two-way ANOVAs were performed to assess the effects of sex and genotype, as well as their interaction: one comparing Control and bGH mice and the other comparing (control) $Ghrhr^{lit}$ and $Ghrhr^{lit/lit}$ mice. Both analyses were followed by Šídák's multiple-comparisons test. A two-way repeated-measures ANOVA, followed by Šídák's multiple-comparisons test, was used to analyze fertility data across the control, bGH, AgRP GHR KO, and AgRP GHR KO/bGH groups. Results with p-values of <0.05 were considered statistically significant.

JNeurosci Accepted Manuscript

RESULTS

Chronic GH excess leads to sexually dimorphic alterations in puberty onset

To investigate whether chronic activation of the somatotropic axis influences reproductive maturation, we assessed pubertal timing in bGH and Ghrhr$^{lit/lit}$ mice. Female bGH and Ghrhr$^{lit/lit}$ mice exhibited vaginal opening and first estrus at ages similar to those of the respective controls, despite significant differences in body weight (Figure 1A-D). In contrast, male bGH and Ghrhr$^{lit/lit}$ mice exhibited delayed pubertal onset, as indicated by later testicular descent and balanopreputial separation compared with control animals (Figure 1E, G). Despite the delayed pubertal onset observed in both models, testosterone levels were similar between bGH and control males during puberty (p=0.2, Table 1). In contrast, pubertal Ghrhr$^{lit/lit}$ mice exhibited higher testosterone levels than their respective controls (p=0.02, Table 1). Male bGH and Ghrhr$^{lit/lit}$ mice exhibited higher and lower body weights, respectively, than control animals at the ages when testicular descent or balanopreputial separation occurred (Figure 1F, H).

Adult bGH mice exhibited increased serum GH and IGF-1 levels, body weight, and nasoanal length, whereas Ghrhr$^{lit/lit}$ animals showed reduced values for these parameters compared with their respective controls (Table 1). In the bGH model, GH and IGF-1 levels showed a significant main effect of genotype (p<0.0001), with no effects of sex or sex × genotype interaction (p>0.05). In the Ghrhr$^{lit/lit}$ model, genotype affected GH levels p<0.0001), whereas IGF-1 levels showed significant effects of sex (p=0.01), genotype (p<0.0001), and sex × genotype interaction (p=0.006). Post hoc analysis indicated that sex differences in heterozygous controls, rather than in Ghrhr$^{lit/lit}$ mice, drove the interaction. These results suggest that changes in the GH/IGF-1 axis impair puberty in mice in a sexually dimorphic manner, with delayed pubertal onset in males despite preserved or even elevated testosterone levels.

Female bGH mice exhibit a disrupted estrous cycle and fertility

JNeurosci Accepted Manuscript

Evaluation of the estrous cycle in adult female mice by vaginal cytology revealed that control mice exhibited a regular 5-day estrous cycle (Figure 2A, D). In contrast, bGH female mice exhibited a prolonged and irregular cycle, characterized by an increased number of days with leukocytes in vaginal lavage ($p < 0.01$; Figure 2B, D). $Ghrhr^{lit/lit}$ females exhibited an estrous cycle of similar duration to that of controls (Figure 2A, C-D). Basal LH and FSH concentrations measured during diestrus were similar in bGH and $Ghrhr^{lit/lit}$ females compared with their respective controls (Figure 2E-F).

Consistent with the observed disrupted estrous cycle, female bGH mice exhibit a pronounced subfertile phenotype, with only 2 out of 10 bGH females achieving pregnancy during the 60-day testing period (Table 2). In contrast, all control females conceived (n = 17). Fertility was preserved in $Ghrhr^{lit/lit}$ females and in male bGH mice (Tables 2 and 3). Together, these findings reveal sex-specific reproductive vulnerability to chronically elevated GH and identify female bGH mice as a model of neuroendocrine subfertility.

GABAergic synaptic input onto kisspeptin neurons is preserved in female bGH mice

Because fertility impairment was evident only in bGH females, subsequent studies focused on this model. To identify central mechanisms underlying infertility, and given the established role of kisspeptin neurons in reproductive control, we next investigated whether kisspeptin neuronal activity is impaired by chronic GH excess. Whole-cell recordings from $AVPV/PeN^{Kisspeptin}$ neurons recorded from bGH mice exhibited RMP and IR values similar to those observed in control females (Table 4). Additionally, spontaneous GABAergic input onto $AVPV/PeN^{Kisspeptin}$ did not differ between bGH (n=10 cells from 5 animals) and control female mice (n=19 cells from 10 animals; $p > 0.05$; Figure 3). Similarly, no significant differences were observed in recordings from $ARH^{Kisspeptin}$ neurons between bGH mice (n=12 cells from 7 animals) and controls (n=16 cells from 10 animals; Table 4, Figure 3). Therefore, basal electrophysiological properties of kisspeptin neurons are preserved during chronic GH elevation.

JNeurosci Accepted Manuscript

Selective GHR ablation in AgRP cells partially restores fertility in female bGH mice

As chemogenetic activation of the AgRP neurons is sufficient to disrupt estrous cyclicity and reduce fertility (Padilla et al., 2017; Coutinho et al., 2020), we next tested whether the subfertility phenotype observed in female bGH mice is mediated by GH action on AgRP neurons. To address this question, we generated a mouse model combining chronic GH hypersecretion with GHR-selective ablation in AgRP-Cre-expressing cells (AgRP GHR KO/bGH). As expected, AgRP GHR KO/bGH mice exhibited increased body weight (30.1 ± 1.5 g) and nasoanal length (9.7 ± 0.2 cm) compared with AgRP GHR KO females (21.0 ± 1.8 g, $p = 0.008$; 7.8 ± 0.5 cm, $p = 0.005$), indicating that selective GHR deletion in AgRP neurons did not prevent the somatic overgrowth induced by chronic GH excess.

Importantly, selective GHR deletion in AgRP neurons substantially improved fertility in GH-hypersecreting females. Approximately seventy-five percent of AgRP GHR KO/bGH females (7 out of 9) achieved pregnancy (Table 2), significantly exceeding the pregnancy rate observed in bGH females (Table 2).

Analysis of reproductive outcomes among control, bGH, and AgRP GHR KO mice revealed a significant main effect of GH hypersecretion on latency to delivery (Table 2, $p = 0.03$), whereas neither genotype nor the interaction between genotype and GH status was statistically significant ($p > 0.05$). In contrast, litter size was significantly influenced by mouse genotype ($p = 0.02$), despite the absence of a main effect of GH hypersecretion and a lack of a significant interaction ($p > 0.05$). Thus, the lack of GH action on AgRP cells, as observed in AgRP GHR KO mice, was sufficient to impair litter size, whereas latency to delivery was influenced by GH hypersecretion, independent of genotype. Together, these findings suggest that GH signaling in AgRP neurons contributes to the reproductive deficits induced by chronic GH excess in female mice.

JNeurosci Accepted Manuscript

GH hypersecretion alters hypothalamic neuropeptide gene expression

To gain further insight into the central mechanisms underlying the reproductive phenotype induced by chronic GH excess, we quantified hypothalamic neuropeptide gene expression involved in metabolic and reproductive functions. Female bGH mice exhibited increased *Agrp* ($p < 0.01$) and decreased *Pomc* mRNA expression ($p < 0.05$; Figure 4A), indicating dysregulation of ARH metabolic circuitry. In addition, *Tac2* mRNA levels were reduced, whereas *Kiss1*, *Gnrh1*, *Pdyn*, *Npy,* or *Esr1* transcripts were unchanged (Figure 4A). These findings suggested that chronic GH excess preferentially targets ARH metabolic neuronal populations rather than disrupting hypothalamic reproductive genes. Notably, hypothalamic *Agrp*, *Pomc,* and *Tac2* mRNA expression were no longer altered in AgRP GHR KO/bGH female compared with respective control (AgRP GHR KO mice, Figure 4B). These results identify AgRP neurons as a critical hypothalamic target mediating the effects of chronic GH excess on neuropeptide gene expression.

GH signaling in AgRP cells contributes to ovarian follicular function

Given that reproductive function depends on the coordinated regulation of the hypothalamic-pituitary-gonadal (HPG) axis, we further investigated whether chronic GH excess is associated with alterations in ovarian follicular dynamics. Ovarian histomorphometry analysis revealed that bGH mice had more primary and secondary follicles than control mice (Figure 5A-B, D). No significant differences were observed in the number of antral follicles (Figure 5A-B, D). However, bGH mice displayed fewer corpora lutea than controls (Figure 5A-B, D, $p < 0.05$). In addition, ovaries from bGH mice showed an increased number of atresic follicles and degenerated retained oocytes, resulting in an overall increase in follicular atresia (Figure 5A-B, E, $p < 0.05$).

Interestingly, the selective deletion of GHR in AgRP cells was sufficient to partially prevent the ovarian dysfunction associated with chronic GH hypersecretion. AgRP GHR KO/bGH female mice exhibited an increased number of antral follicles (Figure 5C, F) and

JNeurosci Accepted Manuscript

405 of atresic follicles (Figure 5G) compared to AgRP GHR KO females, whereas the number
406 of primary and secondary follicles, corpora lutea, and degenerated retained oocytes
407 remained unchanged (Figure 5F, G). Of note, AgRP GHR KO females exhibited ovarian
408 histomorphometric findings comparable to those of control mice (not shown).

409 Together, these findings indicate that GH signaling in AgRP cells contributes, at
410 least in part, to the ovarian dysfunction associated with GH hypersecretion.

JNeurosci Accepted Manuscript

Discussion

Chronic changes in the somatotropic axis have long been associated with reproductive deficits (Advis et al., 1981; Savage et al., 1993; Cecim et al., 1995a; de Boer et al., 1997; Danilovich et al., 1999; Keene et al., 2002; Zaczek et al., 2002; Smuel et al., 2015); however, the central mechanisms underlying these effects remain poorly understood. Here, we demonstrate that sustained GH excess leads to a sexually dimorphic reproductive phenotype and identify AgRP neurons as a key link between somatotropic signaling and female fertility. Chronic GH hypersecretion impaired female fertility, whereas selective deletion of GHR in AgRP neurons substantially improved this deficit, establishing a functional role for this population in mediating the reproductive consequences of GH excess. Contrary to our initial hypothesis, reproductive dysfunction occurs largely independently of overt alterations in canonical kisspeptin neuronal signaling and instead involves coordinated changes in hypothalamic metabolic circuits. These findings indicate that female fertility is vulnerable to sustained alterations in somatotropic signaling. This sex-specific vulnerability may reflect fundamental differences in how metabolic and hormonal cues are integrated within hypothalamic circuits controlling reproduction.

Puberty is a complex physiological process tightly regulated by body weight gain and metabolic cues (Kennedy and Mitra, 1963; Ahmed et al., 2009; Bohlen et al., 2016). Despite marked differences in body weight and GH/IGF-1 secretion, pubertal timing remained preserved in female bGH and $Ghrhr^{lit/lit}$ mice but was delayed in males. Thus, female pubertal onset appears relatively resilient to substantial alterations in somatotropic signaling. Differences in circulating GH and IGF-1 levels between males and females did not appear to account for the divergent pubertal phenotypes observed in homozygous mice. In $Ghrhr^{lit/lit}$ mice, although a sex-by-genotype interaction was detected for IGF-1, post hoc analyses indicated that this interaction primarily reflects differences between male and female $Ghrhr^{lit}$ heterozygous mice rather than between male and female $Ghrhr^{lit/lit}$ mice. Reduced leptin levels have been associated with GH hypersecretion, whereas $Ghrhr^{lit/lit}$

JNeurosci Accepted Manuscript

mice exhibit obesity-associated hyperleptinemia (Berryman et al., 2004; de Paula et al., 2021). Although reduced leptin levels could contribute to delayed pubertal timing in bGH males, this is unlikely to explain the $Ghrhr^{lit/lit}$ mouse phenotype (Berryman et al., 2004; de Paula et al., 2021). Moreover, delayed puberty occurred despite normal testosterone levels in bGH and elevated testosterone levels in $Ghrhr^{lit/lit}$ mice, arguing against a simple testosterone-deficiency mechanism. Thus, both GH/IGF-1 excess and deficiency may affect male pubertal maturation through distinct downstream mechanisms which remain to be determined.

Alterations in GH secretion also differentially affected reproductive capacity between the sexes. GH excess impaired female fertility, whereas male fertility remained unaffected. In females, GH excess disrupted estrous cyclicity without altering gonadotropin concentrations, consistent with previous reports (Debeljuk et al., 1999). Because we did not measure circulating estrogen and progesterone concentrations, we cannot exclude subtle alterations in gonadal steroid signaling. Nevertheless, increased follicular atresia and fewer corpora lutea indicate impaired ovarian function. These effects may reflect changes in HPG-axis dynamics that static hormone measurements do not capture. Because gonadotropin secretion is inherently pulsatile, changes in LH and FSH frequency or amplitude may also occur. Reduced hypothalamic *Tac2* expression observed in bGH females may therefore reflect altered activity of Tac2/neurokinin B-expressing neurons involved in GnRH pulsatility (Lehman et al., 2010). However, because *Tac2* is expressed beyond arcuate KNDy neurons and we analyzed whole hypothalamic tissue, we cannot attribute this finding specifically to kisspeptin neurons (Duarte et al., 2006). Importantly, we found no evidence for major functional impairment in kisspeptin neurons. RMP, IR, and GABAergic synaptic input onto both $AVPV/PeN^{Kisspeptin}$ and $ARH^{Kisspeptin}$ neurons were unchanged by chronic GH excess, and hypothalamic *Kiss1* expression was unaffected. Together with evidence that selective deletion of GHR in kisspeptin-Cre-expressing neurons does not alter pubertal timing or fertility (Bohlen et al., 2019), these findings argue against

JNeurosci Accepted Manuscript

direct GH signaling in kisspeptin neurons as the primary mediator of the reproductive phenotype. Nevertheless, subtle changes in network dynamics, steroid-dependent plasticity, or downstream GnRH secretion cannot be excluded. Elevated GH can also increase prolactin (PRL) secretion, disrupting the PRL surge required for luteal function in mice, compromising fertility (Cecim et al., 1995b; Debeljuk et al., 1999). Although we did not assess PRL dynamics in the present study, altered PRL secretion could contribute to the disrupted estrous cyclicity observed in bGH mice. The absence of changes in *Kiss1* expression, however, argues against profound hyperprolactinemia-associated suppression of kisspeptin signaling (Araujo-Lopes et al., 2014; Brown et al., 2014). Together, these observations suggest that chronic GH excess does not profoundly disrupt canonical kisspeptin signaling under the conditions examined. Because chronic GH excess is accompanied by elevated circulating IGF-1 levels, elevated IGF-1 could influence other neuroendocrine populations, including GnRH neurons (Divall et al., 2010). Moreover, the intraovarian effects of chronic GH/IGF-1 excess on follicular dynamics cannot be ruled out, as evidenced by an increased population of primordial and secondary follicles that is independent of gonadotropins (Wu et al., 2023).

Notably, our findings support an important role for AgRP neurons in the neuroendocrine mechanisms linking somatotropin activity to reproduction. Selective GHR deletion in AgRP neurons substantially improved female fertility and prevented the transcriptional remodeling induced by chronic GH excess, further supporting the role of this neuronal population in GH's reproductive effects. Consistent with this effect, bGH female mice exhibited increased *Agrp* and reduced *Pomc* and *Tac2* expression, suggesting that chronic GH excess alters transcriptional programs related to ARH neuropeptide signaling. Interestingly, genetic deletion of *Agrp* has been shown to increase hypothalamic *Tac2* expression, while pharmacological MC4R activation stimulates TAC2 neurons, suggesting functional interactions between AgRP/melanocortin and the Tac2/KNDy pathways (Sheffer-Babila et al., 2013). However, because these measurements were performed in the whole

JNeurosci Accepted Manuscript

hypothalamus, the transcriptional changes observed in the bGH model cannot be assigned to specific neuronal populations. The absence of transcriptional alterations in AgRP GHR KO/bGH mice nevertheless supports AgRP neurons as a critical mediator of GH-induced hypothalamic remodeling. This effect is notable because the reproductive phenotype occurred without a classical energy-deficient state, suggesting that chronic GH excess may alter central metabolic sensing independently of peripheral energy stores. Together, these findings support a role for AgRP neurons in the neuroendocrine mechanism linking somatotropin activity to reproduction. Accordingly, our data extend previous evidence that manipulation of AgRP neuronal activity influences fertility (Egan et al., 2017; Padilla et al., 2017; Coutinho et al., 2020). This interpretation is consistent with studies showing that ablation of AgRP neurons restores fertility in leptin-deficient (ob/ob) mice. In contrast, similar manipulations targeting melanin-concentrating hormone-expressing neurons do not produce comparable effects (Wu et al., 2012). Given that POMC neurons are GH-responsive and regulate fertility through MC4R-dependent signaling in kisspeptin neurons, a partial contribution of this neuronal population cannot be excluded (Quaresma et al., 2019; Talbi et al., 2025).

The incomplete rescue of fertility in AgRP GHR KO/bGH females indicates that additional mechanisms contribute to GH-induced reproductive dysfunction. Ovarian dysfunction appears to be an important component, although direct ovarian effects cannot be distinguished from systemic or neuroendocrine mechanisms. Fewer corpora lutea may reflect inadequate endocrine stimulation of ovulation, although impaired follicular competence cannot be excluded. Partial restoration of ovarian morphology after GHR deletion in AgRP neurons supports a contribution of GH-responsive hypothalamic circuits. Autonomic pathways may also contribute, as AgRP neurons influence autonomic output and the ovary receives sympathetic and parasympathetic innervation (Uchida and Kagitani, 2015; Bell et al., 2018). The mechanisms underlying this hypothalamic-ovarian interaction warrant further investigation.

JNeurosci Accepted Manuscript

519 Elevated circulating IGF-1 levels have also been reported in women and animal
520 models of polyendocrine metabolic ovarian syndrome (PMOS), a common cause of
521 anovulatory infertility (Ruiz et al., 1997; Berker et al., 2004; Li et al., 2023). Findings
522 regarding GH secretion in PMOS are inconsistent, with reports of normal or elevated GH
523 secretion (Garcia-Rudaz et al., 2002; Premoli et al., 2005). Although speculative, these
524 observations suggest that increased GH/IGF-1 signaling may contribute to female
525 reproductive dysfunction through coordinated hypothalamic and ovarian mechanisms, as
526 both tissues express GHR and IGF1R (Lobie et al., 1990; Baumgarten et al., 2017).
527 Because GH excess is accompanied by marked IGF-1 elevations (Wasinski et al., 2023), it
528 remains unclear whether GH, IGF-1, or both mediate the observed effects. Moreover,
529 hypothalamic IGF-1 resistance under metabolic stress raises the possibility that altered
530 central IGF-1 responsiveness contributes to the hypothalamic adaptations observed in bGH
531 mice, although this hypothesis remains to be investigated (He et al., 2025).

532 In conclusion, our findings uncover a previously unrecognized sexually dimorphic
533 role of GH signaling in the control of reproduction. Whereas both GH excess and deficiency
534 similarly affected male pubertal development, sustained GH hypersecretion selectively
535 impaired female fertility. Our data indicate that this phenotype is associated with remodeling
536 of hypothalamic metabolic neurocircuitry, partly mediated by AgRP neurons, and ovarian
537 dysfunction, rather than overt alterations in canonical kisspeptin neuronal function.
538 Furthermore, the substantial rescue observed following GHR deletion in AgRP cells
539 identifies this population as a major neural substrate linking somatotropic and reproductive
540 function. Together, these findings advance our understanding of how chronic alterations in
541 GH/IGF-1 homeostasis influence female fertility and establish AgRP neurons as a
542 neuroendocrine interface through which metabolic and reproductive signals integrate.

JNeurosci Accepted Manuscript

REFERENCES

Advis JP, White SS, Ojeda SR (1981) Activation of growth hormone short loop negative feedback delays puberty in the female rat. Endocrinology 108:1343-1352.

Ahmed ML, Ong KK, Dunger DB (2009) Childhood obesity and the timing of puberty. Trends in Endocrinology & Metabolism 20:237-242.

Anderson GM, Hill JW, Kaiser UB, Navarro VM, Ong KK, Perry JRB, Prevot V, Tena-Sempere M, Elias CF (2024) Metabolic control of puberty: 60 years in the footsteps of Kennedy and Mitra's seminal work. Nat Rev Endocrinol 20:111-123.

Araujo-Lopes R, Crampton JR, Aquino NS, Miranda RM, Kokay IC, Reis AM, Franci CR, Grattan DR, Szawka RE (2014) Prolactin regulates kisspeptin neurons in the arcuate nucleus to suppress LH secretion in female rats. Endocrinology 155:1010-1020.

Backholer K, Smith JT, Rao A, Pereira A, Iqbal J, Ogawa S, Li Q, Clarke IJ (2010) Kisspeptin cells in the ewe brain respond to leptin and communicate with neuropeptide Y and proopiomelanocortin cells. Endocrinology 151:2233-2243.

Bartke A (1999) Role of growth hormone and prolactin in the control of reproduction: What are we learning from transgenic and knock-out animals?1. Steroids 64:598-604.

Baumgarten SC, Armouti M, Ko C, Stocco C (2017) IGF1R Expression in Ovarian Granulosa Cells Is Essential for Steroidogenesis, Follicle Survival, and Fertility in Female Mice. Endocrinology 158:2309-2318.

Bell BB, Harlan SM, Morgan DA, Guo DF, Cui H, Rahmouni K (2018) Differential contribution of POMC and AgRP neurons to the regulation of regional autonomic nerve activity by leptin. Mol Metab 8:1-12.

Berker B, Emral R, Demirel C, Corapcioglu D, Unlu C, Kose K (2004) Increased insulin-like growth factor-I levels in women with polycystic ovary syndrome, and beneficial effects of metformin therapy. Gynecol Endocrinol 19:125-133.

Berryman DE, List EO, Coschigano KT, Behar K, Kim JK, Kopchick JJ (2004) Comparing adiposity profiles in three mouse models with altered GH signaling. Growth hormone & IGF research : official journal of the Growth Hormone Research Society and the International IGF Research Society 14:309-318.

Bohlen TM, Silveira MA, Zampieri TT, Frazao R, Donato J, Jr. (2016) Fatness rather than leptin sensitivity determines the timing of puberty in female mice. Mol Cell Endocrinol 423:11-21.

Bohlen TM, Zampieri TT, Furigo IC, Teixeira PD, List EO, Kopchick J, Donato J, Jr., Frazao R (2019) Central growth hormone signaling is not required for the timing of puberty. J Endocrinol:JOE-19-0242.

Brown RS, Herbison AE, Grattan DR (2014) Prolactin regulation of kisspeptin neurones in the mouse brain and its role in the lactation-induced suppression of kisspeptin expression. J Neuroendocrinol 26:898-908.

Cecim M, Kerr J, Bartke A (1995a) Effects of bovine growth hormone (bGH) transgene expression or bGH treatment on reproductive functions in female mice. Biol Reprod 52:1144-1148.

Cecim M, Fadden C, Kerr J, Steger RW, Bartke A (1995b) Infertility in Transgenic Mice Overexpressing the Bovine Growth Hormone Gene: Disruption of the Neuroendocrine Control of Prolactin Secretion during Pregnancy1. Biology of Reproduction 52:1187-1192.

Coutinho EA, Prescott M, Hessler S, Marshall CJ, Herbison AE, Campbell RE (2020) Activation of a Classic Hunger Circuit Slows Luteinizing Hormone Pulsatility. Neuroendocrinology 110:671-687.

Danilovich N, Wernsing D, Coschigano KT, Kopchick JJ, Bartke A (1999) Deficits in Female Reproductive Function in GH-R-KO Mice; Role of IGF-I. Endocrinology 140:2637-2640.

JNeuroendocrinol Accepted Manuscript

595 de Boer JA, Schoemaker J, van der Veen EA (1997) Impaired reproductive function in
596 women treated for growth hormone deficiency during childhood. Clin Endocrinol
597 (Oxf) 46:681-689.
598 de Oliveira LS, da Silva TQM, Barbosa EM, dos Anjos Cordeiro JM, Santos LC,
599 Henriques PC, Santos BR, Gusmao DdO, de Macedo IO, Szawka RE, Silva JF
600 (2022) Kisspeptin Treatment Restores Ovarian Function in Rats with
601 Hypothyroidism. Thyroid® 32:1568-1579.
602 de Paula DG, Bohlen TM, Zampieri TT, Mansano NS, Vieira HR, Gusmao DO, Wasinski
603 F, Donato J, Jr., Frazao R (2021) Distinct effects of growth hormone deficiency
604 and disruption of hypothalamic kisspeptin system on reproduction of male mice.
605 Life sciences 285:119970.
606 de Sousa LMM, Vicente VAN, Donato J, Jr. (2025) Negative Feedback Loops and
607 Hormonal Factors that Regulate GH Secretion. Endocrinology 166.
608 Debeljuk L, Steger RW, Wright JC, Mattison J, Bartke A (1999) Effects of overexpression
609 of growth hormone-releasing hormone on the hypothalamo-pituitary-gonadal
610 function in the mouse. Endocrine 11:171-179.
611 Divall SA, Williams TR, Carver SE, Koch L, Brüning JC, Kahn CR, Wondisford F,
612 Radovick S, Wolfe A (2010) Divergent roles of growth factors in the GnRH
613 regulation of puberty in mice. The Journal of clinical investigation 120:2900-2909.
614 Donato J, Jr., Wasinski F, Furigo IC, Metzger M, Frazão R (2021) Central Regulation of
615 Metabolism by Growth Hormone. Cells 10.
616 Donato J, Jr., Cravo RM, Frazao R, Gautron L, Scott MM, Lachey J, Castro IA, Margatho
617 LO, Lee S, Lee C, Richardson JA, Friedman J, Chua S, Jr., Coppari R, Zigman
618 JM, Elmquist JK, Elias CF (2011) Leptin's effect on puberty in mice is relayed by
619 the ventral premammillary nucleus and does not require signaling in Kiss1
620 neurons. J Clin Invest 121:355-368.
621 Duarte CR, Schütz B, Zimmer A (2006) Incongruent pattern of neurokinin B expression in
622 rat and mouse brains. Cell Tissue Res 323:43-51.
623 Egan OK, Inglis MA, Anderson GM (2017) Leptin Signaling in AgRP Neurons Modulates
624 Puberty Onset and Adult Fertility in Mice. J Neurosci 37:3875-3886.
625 Farias Quipildor G, Mao K, Beltran PJ, Barzilai N, Huffman DM (2021) Modulation of
626 Glucose Production by Central Insulin Requires IGF-1 Receptors in AgRP
627 Neurons. Diabetes 70:2237-2249.
628 Frazao R, Lemko HMD, da Silva RP, Ratra DV, Lee CE, Williams KW, Zigman JM, Elias
629 CF (2014) Estradiol modulates Kiss1 neuronal response to ghrelin. American
630 Journal of Physiology - Endocrinology And Metabolism 306:E606-E614.
631 Furigo IC, Teixeira PDS, de Souza GO, Couto GCL, Romero GG, Perelló M, Frazão R,
632 Elias LL, Metzger M, List EO, Kopchick JJ, J D (2019) Growth hormone regulates
633 neuroendocrine responses to weight loss via AgRP neurons. Nature
634 communications 10:662.
635 Garcia-Rudaz MC, Ropelato MG, Escobar ME, Veldhuis JD, Barontini M (2002) Amplified
636 and orderly growth hormone secretion characterizes lean adolescents with
637 polycystic ovary syndrome. European journal of endocrinology / European
638 Federation of Endocrine Societies 147:207-216.
639 Gusmao DO, Vieira HR, Mansano NS, Tavares MR, de Sousa LMM, Wasinski F, Frazao
640 R, Donato J, Jr. (2022) Pattern of gonadotropin secretion along the estrous cycle
641 of C57BL/6 female mice. Physiol Rep 10:e15460.
642 He W, Loganathan N, Belsham DD (2025) IGF1 Signaling Regulates Neuropeptide
643 Expression in Hypothalamic Neurons Under Physiological and Pathological
644 Conditions. Endocrinology 166.
645 Inoue S, Watanabe H, Saito H, Hiroi M, Tonosaki A (2000) Elimination of atretic follicles
646 from the mouse ovary: a TEM and immunohistochemical study in mice. Journal of
647 Anatomy 196:103-110.

JNeuroscAccepted Manuscript

Keene DE, Suescun MO, Bostwick MG, Chandrashekar V, Bartke A, Kopchick JJ (2002) Puberty Is Delayed in Male Growth Hormone Receptor Gene—Disrupted Mice. Journal of Andrology 23:661-668.

Kennedy GC, Mitra J (1963) Body weight and food intake as initiating factors for puberty in the rat. J Physiol 166:408-418.

Krashes MJ, Koda S, Ye C, Rogan SC, Adams AC, Cusher DS, Maratos-Flier E, Roth BL, Lowell BB (2011) Rapid, reversible activation of AgRP neurons drives feeding behavior in mice. The Journal of Clinical Investigation 121:1424-1428.

Lehman MN, Coolen LM, Goodman RL (2010) Minireview: kisspeptin/neurokinin B/dynorphin (KNDy) cells of the arcuate nucleus: a central node in the control of gonadotropin-releasing hormone secretion. Endocrinology 151:3479-3489.

Lehman MN et al. (2018) The 3(rd) World Conference on Kisspeptin, "Kisspeptin 2017: Brain and Beyond":Unresolved questions, challenges and future directions for the field. J Neuroendocrinol 30:e12600.

Li H, Zhang Y, Liu C, Zhang Y, Yang H, Fu S, Lv H (2023) Association of Insulin-Like Growth Factor-1 With Polycystic Ovarian Syndrome: A Systematic Review and Meta-analysis. Endocrine Practice 29:388-397.

List EO, Berryman DE, Funk K, Gosney ES, Jara A, Kelder B, Wang X, Kutz L, Troike K, Lozier N, Mikula V, Lubbers ER, Zhang H, Vesel C, Junnila RK, Frank SJ, Masternak MM, Bartke A, Kopchick JJ (2013) The role of GH in adipose tissue: lessons from adipose-specific GH receptor gene-disrupted mice. Mol Endocrinol 27:524-535.

List EO, Berryman DE, Funk K, Jara A, Kelder B, Wang F, Stout MB, Zhi X, Sun L, White TA, LeBrasseur NK, Pirtskhalava T, Tchkonia T, Jensen EA, Zhang W, Masternak MM, Kirkland JL, Miller RA, Bartke A, Kopchick JJ (2014) Liver-specific GH receptor gene-disrupted (LiGHRKO) mice have decreased endocrine IGF-I, increased local IGF-I, and altered body size, body composition, and adipokine profiles. Endocrinology 155:1793-1805.

Lobie PE, Breipohl W, Aragón JG, Waters MJ (1990) Cellular localization of the growth hormone receptor/binding protein in the male and female reproductive systems. Endocrinology 126:2214-2221.

Manfredi-Lozano M, Roa J, Ruiz-Pino F, Piet R, Garcia-Galiano D, Pineda R, Zamora A, Leon S, Sanchez-Garrido MA, Romero-Ruiz A, Dieguez C, Vazquez MJ, Herbison AE, Pinilla L, Tena-Sempere M (2016) Defining a novel leptin-melanocortin-kisspeptin pathway involved in the metabolic control of puberty. Mol Metab 5:844-857.

Mansano NDS, Vieira HR, Araujo-Lopes R, Szawka RE, Donato J, Jr., Frazao R (2023) Fasting Modulates GABAergic Synaptic Transmission to Arcuate Kisspeptin Neurons in Female Mice. Endocrinology 164.

Meng L, Rijntjes E, Swarts HJ, Keijer J, Teerds KJ (2017) Prolonged hypothyroidism severely reduces ovarian follicular reserve in adult rats. J Ovarian Res 10:19.

Merkley CM, Shuping SL, Sommer JR, Nestor CC (2021) Evidence That Agouti-Related Peptide May Directly Regulate Kisspeptin Neurons in Male Sheep. Metabolites 11.

Nestor CC, Qiu J, Padilla SL, Zhang C, Bosch MA, Fan W, Aicher SA, Palmiter RD, Rønnekleiv OK, Kelly MJ (2016) Optogenetic Stimulation of Arcuate Nucleus Kiss1 Neurons Reveals a Steroid-Dependent Glutamatergic Input to POMC and AgRP Neurons in Male Mice. Mol Endocrinol 30:630-644.

Padilla SL, Qiu J, Nestor CC, Zhang C, Smith AW, Whiddon BB, Ronnekleiv OK, Kelly MJ, Palmiter RD (2017) AgRP to Kiss1 neuron signaling links nutritional state and fertility. Proc Natl Acad Sci U S A 114:2413-2418.

Premoli AC, Santana LF, Ferriani RA, de Moura MD, Silva De Sá MF, dos Reis RM (2005) Growth hormone secretion and insulin-like growth factor-1 are related to hyperandrogenism in nonobese patients with polycystic ovary syndrome. Fertility and sterility 83:1852-1855.

JNeurosci Accepted Manuscript

Qiu J, Rivera HM, Bosch MA, Padilla SL, Stincic TL, Palmiter RD, Kelly MJ, Ronnekleiv OK (2018) Estrogenic-dependent glutamatergic neurotransmission from kisspeptin neurons governs feeding circuits in females. Elife 7.

Quaresma PGF, Teixeira PDS, Furigo IC, Wasinski F, Couto GC, Frazão R, List EO, Kopchick JJ, Donato J (2019) Growth hormone/STAT5 signaling in proopiomelanocortin neurons regulates glucoprivic hyperphagia. Molecular and Cellular Endocrinology 498:110574.

Ranke MB, Wit JM (2018) Growth hormone - past, present and future. Nat Rev Endocrinol 14:285-300.

Ross RA, Leon S, Madara JC, Schafer D, Fergani C, Maguire CA, Verstegen AM, Brengle E, Kong D, Herbison AE, Kaiser UB, Lowell BB, Navarro VM (2018) PACAP neurons in the ventral premammillary nucleus regulate reproductive function in the female mouse. Elife 7:e35960.

Ruiz A, Tébar M, Pérez-Romero A, Rol de Lama MA, Sánchez-Criado JE (1997) Serum levels of GH, IGF-I, LH and ovarian steroids in cyclic and RU486-treated rats. J Endocrinol Invest 20:611-615.

Savage MO, Blum WF, Ranke MB, Postel-Vinay MC, Cotterill AM, Hall K, Chatelain PG, Preece MA, Rosenfeld RG (1993) Clinical features and endocrine status in patients with growth hormone insensitivity (Laron syndrome). J Clin Endocrinol Metab 77:1465-1471.

Sheffer-Babila S, Sun Y, Israel DD, Liu SM, Neal-Perry G, Chua SC, Jr. (2013) Agouti-related peptide plays a critical role in leptin's effects on female puberty and reproduction. Am J Physiol Endocrinol Metab 305:E1512-1520.

Silva JDN, de Sousa LMM, de Sousa ME, Vieira HR, Alves GA, Neifert NT, Moore AM, Donato J, Jr., Frazao R (2026) KNDy neurons as an indirect target of insulin-like growth factor-1. J Neuroendocrinol 38:e70130.

Silveira MA, Zampieri TT, Furigo IC, Abdulkader F, Donato J, Jr., Frazao R (2019) Acute effects of somatomammotropin hormones on neuronal components of the hypothalamic-pituitary-gonadal axis. Brain Res 1714:210-217.

Silveira MA, Furigo IC, Zampieri TT, Bohlen TM, de Paula DG, Franci CR, Donato J, Jr., Frazao R (2017) STAT5 signaling in kisspeptin cells regulates the timing of puberty. Mol Cell Endocrinol 448:55-65.

Smuel K, Kauli R, Lilos P, Laron Z (2015) Growth, development, puberty and adult height before and during treatment in children with congenital isolated growth hormone deficiency. Growth hormone & IGF research : official journal of the Growth Hormone Research Society and the International IGF Research Society 25:182-188.

Steyn FJ, Tolle V, Chen C, Epelbaum J (2016) Neuroendocrine Regulation of Growth Hormone Secretion. Compr Physiol 6:687-735.

Steyn FJ, Wan Y, Clarkson J, Veldhuis JD, Herbison AE, Chen C (2013) Development of a methodology for and assessment of pulsatile luteinizing hormone secretion in juvenile and adult male mice. Endocrinology 154:4939-4945.

Stincic TL, Qiu J, Connors AM, Kelly MJ, Rønnekleiv OK (2021) Arcuate and Preoptic Kisspeptin Neurons Exhibit Differential Projections to Hypothalamic Nuclei and Exert Opposite Postsynaptic Effects on Hypothalamic Paraventricular and Dorsomedial Nuclei in the Female Mouse. eNeuro 8.

Talbi R, Stincic TL, Ferrari K, Ji Hae C, Walec K, Medve E, Gerutshang A, Leon S, McCarthy EA, Rønnekleiv OK, Kelly MJ, Navarro VM (2025) POMC neurons control fertility through differential signaling of MC4R in kisspeptin neurons. eLife 13:RP100722.

Uchida S, Kagitani F (2015) Autonomic nervous regulation of ovarian function by noxious somatic afferent stimulation. The Journal of Physiological Sciences 65:1-9.

Wasinski F, Tavares MR, Gusmao DO, List EO, Kopchick JJ, Alves GA, Frazao R, Donato J, Jr. (2023) Central growth hormone action regulates neuroglial and

JNeurosci Accepted Manuscript

proinflammatory markers in the hypothalamus of male mice. Neurosci Lett 806:137236.

Wu GMJ, Chen ACH, Yeung WSB, Lee YL (2023) Current progress on in vitro differentiation of ovarian follicles from pluripotent stem cells. Front Cell Dev Biol 11:1166351.

Wu Q, Whiddon BB, Palmiter RD (2012) Ablation of neurons expressing agouti-related protein, but not melanin concentrating hormone, in leptin-deficient mice restores metabolic functions and fertility. Proc Natl Acad Sci U S A 109:3155-3160.

Zaczek D, Hammond J, Suen L, Wandji S, Service D, Bartke A, Chandrashekar V, Coschigano K, Kopchick J (2002) Impact of Growth Hormone Resistance on Female Reproductive Function: New Insights from Growth Hormone Receptor Knockout Mice1. Biology of Reproduction 67:1115-1124.

JNeurosci Accepted Manuscript

Figure 1- GH effects on puberty onset. (A–H) Bar graphs illustrating average age of vaginal opening (VO), first estrus (1st estrus), testicular descent (TD), balanopreputial separation (BPS), and the average body weight at specific ages when puberty events were observed in bGH, and Ghrhr$^{lit/lit}$ mice (n=4/25 per group). * Significant difference compared with the respective control group; *** $p < 0.001$; **** $p < 0.0001$. Unpaired two-tailed Student's t-test or Mann–Whitney test.

Figure 2- GH effects on estrous cycle and gonadotropin levels. (A–C) Representative graphs showing estrous cyclicity of control (A), bGH (B), and Ghrhr$^{lit/lit}$ mice (C). (D–F) Bar graphs illustrating estrous cycle length (D), luteinizing hormone (LH, E), and follicle-stimulating hormone serum levels (FSH, F) of control, bGH, and Ghrhr$^{lit/lit}$ mice (n=4/8 per group). For estrous cyclicity quantification, a period between the first day on which cornified cells were observed in the vaginal smear, the transition to leukocytes, and the next day on which cornified cells reappeared was considered a complete estrous cycle. Abbreviations: P/E, proestrus and estrus; M/D, metestrus and diestrus. *Significant difference compared with the respective control group; ** $p < 0.01$. Unpaired two-tailed Student's t-test or Mann–Whitney test.

Figure 3- Effects of GH excess on GABAergic synaptic transmission to kisspeptin neurons. Whole-cell recordings were performed in kisspeptin neurons located in the anteroventral periventricular and rostral periventricular nuclei (AVPV/PeN, A-C) or in the arcuate nucleus of the hypothalamus (ARH, D-F). (A, D) Representative voltage-clamp traces showing GABAergic postsynaptic currents recorded from ex vivo hypothalamic slices obtained from control or bGH females. (B–C, E–F) Bar graphs showing the average frequency (B, E) or amplitude (C, F) of GABAergic postsynaptic currents in kisspeptin neurons from control and bGH female mice in the AVPV/PeN (B-C) and ARH (E-F). Unpaired two-tailed Student's t-test.

Figure 4 - Effects of GH excess on hypothalamic mRNA expression. (A-B) Bar graphs showing average hypothalamic mRNA expression of *Agrp*, *Npy*, *Pomc, Kiss1*, *Gnrh1*, *Tac2*, *Pdyn*, and *Esr1* genes in bGH versus control female mice (A), or in AgRP GHR KO/bGH versus control (AgRP-CRE GHR KO) female mice (B). *Significant difference compared with the respective control group; ** $p < 0.01$; **** $p < 0.0001$. Unpaired two-tailed Student's t-test.

Figure 5 – Chronic GH excess effects on ovarian morphology. (A–C) Representative ovarian sections stained with hematoxylin and eosin from control (A), bGH (B), and AgRP GHR KO/bGH (C) mice. (D-G) Bar graphs showing the quantification of the primary follicles, secondary follicles, antral follicles, and corpora lutea (CL) (D, F), atretic follicles, degenerated retained oocytes, and total atretic follicles (E, G) of control and bGH mice (D-E, n=5/6 per group), or AgRP GHR KO and AgRP GHR KO/bGH mice (F, G, n=5/6 per group). Scale bar, 50 µm. Unpaired two-tailed Student's t-test, $p > 0.05$.

JNeurosci Accepted Manuscript

Table 1- Sex-specific effects of GH excess or deficiency on mouse growth

	Female		***Male***	
	Control	**bGH**	**Control**	**bGH**
GH (ng/ml)	4.4 ± 1.8 (n=5)	13.5 ± 0.7*** (n=6)	5.7 ± 1.9 (n=8)	13.7 ± 0.4** (n=8)
IGF-1 (ng/ml)	427.4 ± 18.3 (n=5)	944.9 ± 23.5**** (n=6)	419.5 ± 24.3 (n=8)	940.9 ± 31.7**** (n=8)
Testosterone (ng/ml)	-	-	0.22 ± 0.02 (n=6)	0.19 ± 0.02 (n=5)
Body weight (g)	24.1 ± 0.5 (n=10)	37.3 ± 1.4**** (n=10)	26.7 ± 0.5 (n=10)	41.5 ± 0.9**** (n=10)
Nasoanal length (cm)	9.2 ± 0.3 (n=9)	10.9 ± 0.4** (n=9)	9.1 ± 0.1 (n=10)	10.9 ± 0.3**** (n=10)
Uterine relative weight (% body weight)	0.3 ± 0.1 (n=5)	0.2 ± 0.1 (n=5)	-	-
	Control	**Ghrhr$^{lit/lit}$**	**Control**	**Ghrhr$^{lit/lit}$**
GH (ng/ml)	4.4 ± 2.7 (n=4)	0.5 ± 0.1$^{\#}$ (n=7)	13.6 ± 4.7 (n=5)	0.0 ± 0.0* (n=4)
IGF-1 (ng/ml)	408.9 ± 21.7 (n=4)	20.3 ± 1.3** (n=7)	327.4 ± 20.2 (n=5)	23.7 ± 3.6* (n=4)
Testosterone (ng/ml)	-	-	0.34 ± 0.04 (n=6)	0.60 ± 0.08* (n=6)
Body weight (g)	22.2 ± 1.0 (n=10)	10.7 ± 0.6**** (n=10)	24.8 ± 0.7 (n=10)	14.1 ± 0.6**** (n=10)
Nasoanal length (cm)	8.9 ± 0.2 (n=7)	6.7 ± 0.2**** (n=8)	10.1 ± 0.4 (n=4)	7.4 ± 0.3** (n=4)
Uterine relative weight (% body weight)	0.3 ± 0.1 (n=3)	0.4 ± 0.1% (n=4)	-	-

Data are expressed as mean ± standard error. Unless otherwise indicated, all parameters were measured in adult mice, whereas testosterone concentrations were measured in pubertal mice (28-30 days of age). We assessed statistical significance using an unpaired two-tailed Student's t-test or Mann–Whitney test. * $p < 0.05$; ** $p < 0.01$; *** $p < 0.001$; **** $p < 0.0001$, versus the respective Control group. For GH and IGF-1 concentrations, we analyzed sex and genotype, as well as their interaction, using two-way ANOVA followed by Šidak's multiple-comparisons test. For bGH mice, GH and IGF-1 concentrations showed: sex, p>0.05; genotype, p<0.0001; sex x genotype interaction, p>0.05; post hoc comparison, p>0.05. For Ghrhr$^{lit/lit}$ mice, GH concentrations: sex, p>0.05; genotype, p=0.004; sex vs genotype interaction, p>0.05; post hoc comparison, p>0.05. For IGF-1 concentrations, sex, p=0.1; genotype, p<0.0001; sex vs genotype interaction, p=0.006; post hoc comparison, p>0.05, except for Ghrhr^{lit}, p=0.002.

JNeurosci Accepted Manuscript

Table 2- Female reproductive function

	Control	**bGH**
Fertility rate (%)	100% (n=17)	20% (n= 2 out of 10) ****
Days until birth	23.3 ± 1.5 (n=17)	34.0 ± 12.0^{+} (n=2)
Litter size	6.4 ± 0.3 (n=17)	6.5 ± 2.5 (n=2)
	AgRP GHR KO	**AgRP GHR KO/bGH**
Fertility rate (%)	100% (n=10)	75% (n=7 out of 9)
Days until birth	27.2 ± 2.3 (n=10)	37.4 ± 7.8^{+} (n=5)
Litter size	4.7 ± 0.5$^{\$}$ (n=10)	4.0 ± 1.0$^{\$}$ (n=4)
	Control	**Ghrhr$^{lit/lit}$**
Fertility rate (%)	90% (n=8 out of 9)	100% (n=6)
Days until birth	23.6± 0.9 (n=8)	25.8 ± 1.1 (n=6)
Litter size	6.9 ± 0.6 (n=8)	4.4 ± 0.4** (n=6)

Continuous data are presented as mean ± SEM, whereas fertility rate is presented as a percentage. We evaluated fertility rate by Fisher's exact test, **** $p < 0.001$. Comparison among control, bGH, AgRP GHR KO, and AgRP GHR KO/bGH was performed using two-way repeated-measures ANOVA, followed by Šidak's multiple-comparison test; $^{+}$ $p < 0.05$, main effect of GH levels; $^{\$}$ $p < 0.05$, main effect of genotype. For the AgRP GHR KO/bGH group, sample sizes differed among outcomes because one litter was lost, and birth date and litter size data were unavailable for two additional litters. Thus, we analyzed n = 9 litters for fertility rate, n = 5 for days until birth, and n = 4 for litter size. We compared Ghrhr$^{lit/lit}$ and control data using an unpaired two-tailed Student's t-test or the Mann–Whitney test. $p > 0.05$.

JNeurosci Accepted Manuscript

842 Table 3- Male reproductive function

Male	**Control**	**bGH**
Fertility rate (%)	84% (n= 11 out of 13)	72% (n= 8 out of 11)
Days until birth	25.7 ± 2.0 (n=11)	33.0 ± 6.5 (n=8)
Litter size	5.6 ± 0.7 (n=11)	5.5 ± 0.4 (n=8)

843 Data are expressed as mean ± standard error. We evaluated fertility rate by Fisher's exact
844 test. We analyzed the remaining data using an unpaired two-tailed Student's t-test or the
845 Mann–Whitney test. $p > 0.05$.
846
847

848

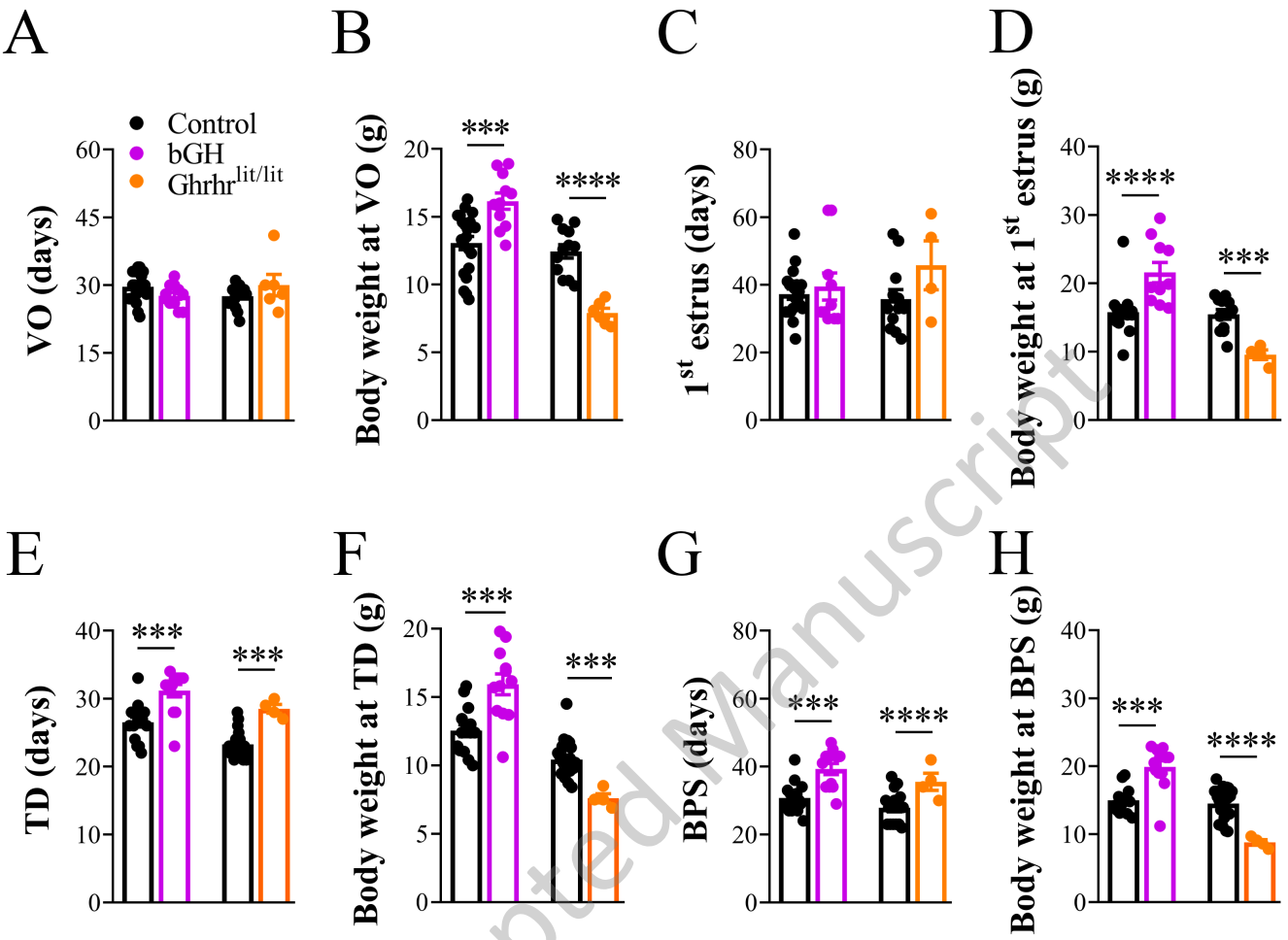
JNeurosci Accepted Manuscript

Table 4- GH excess effect on kisspeptin neurons' biophysical properties

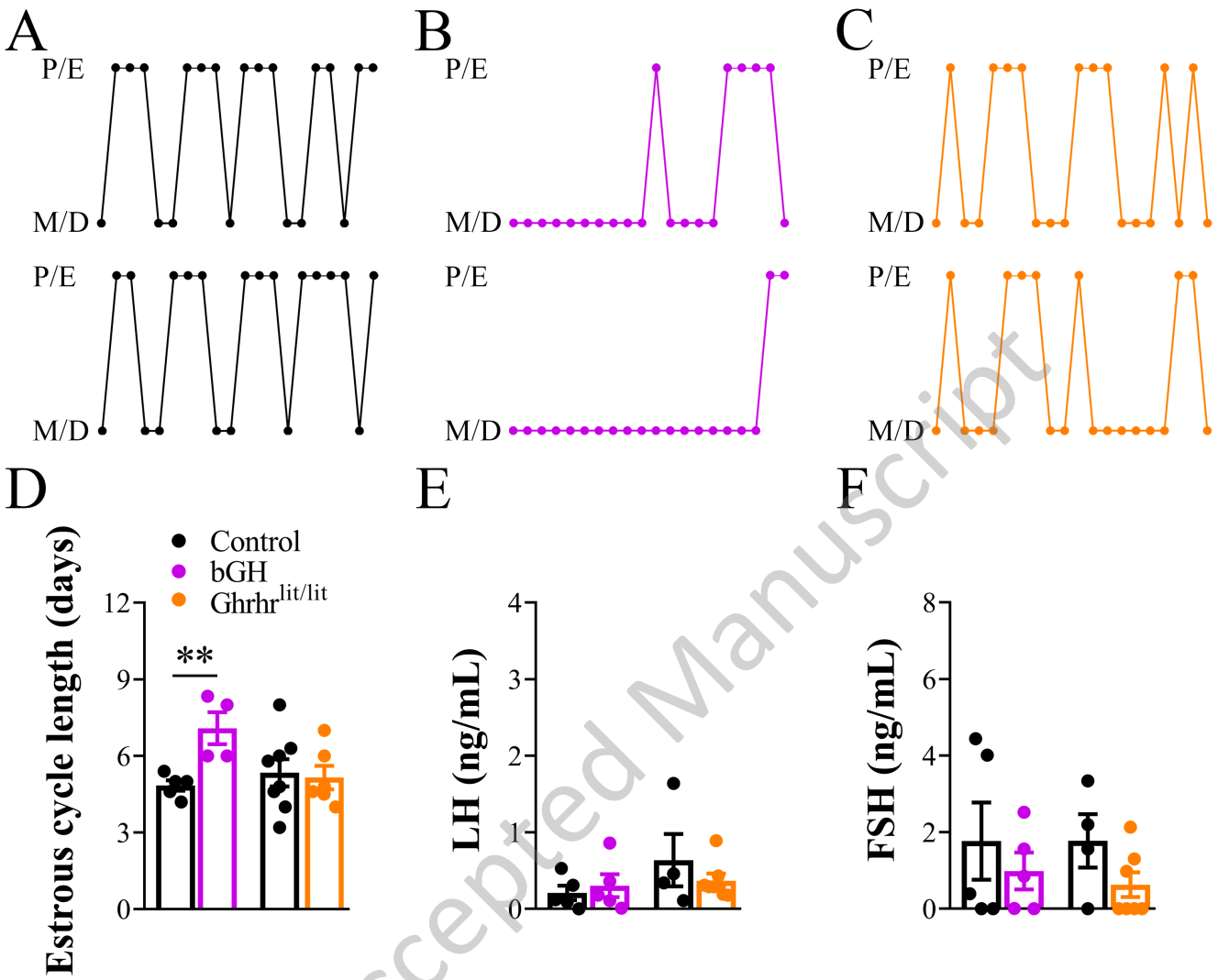
	Female	
AVPV/PeN^{Kisspeptin}	**Control**	**bGH**
RMP (mV)	-74.0 ± 1.3 (n=28)	-77.3 ± 2.4 (n=13)
IR (GΩ)	0.5 ± 0.1 (n=28)	0.7 ±0.1 (n=13)
ARH^{Kisspeptin}		
RMP (mV)	-58.0 ± 1.3 (n=36)	-62.5 ± 4.8 (n=16)
IR (GΩ)	1.4 ± 0.1 (n=36)	1.4 ± 0.1 (n=16)

Data are expressed as mean ± standard error (4/10 mice per group). Statistical significance was determined using an unpaired two-tailed Student's t-test.

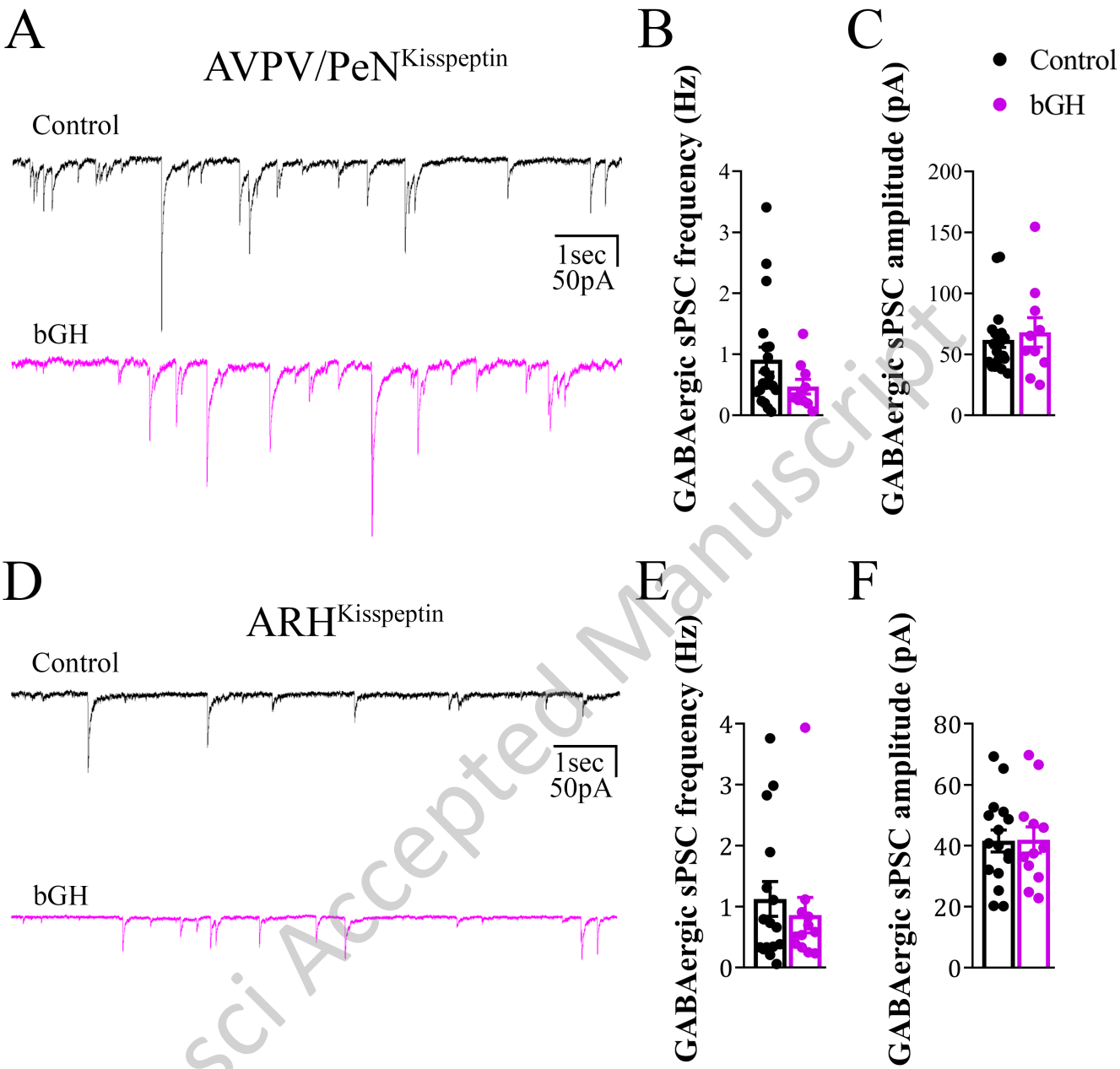
JNeurosci Accepted Manuscript



JNeurosci Accepted Manuscript

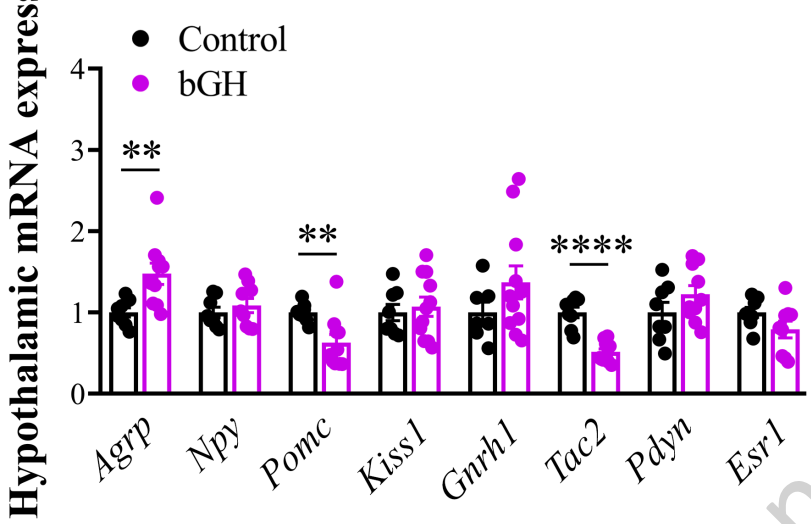


JNeurosci Accepted Manuscript

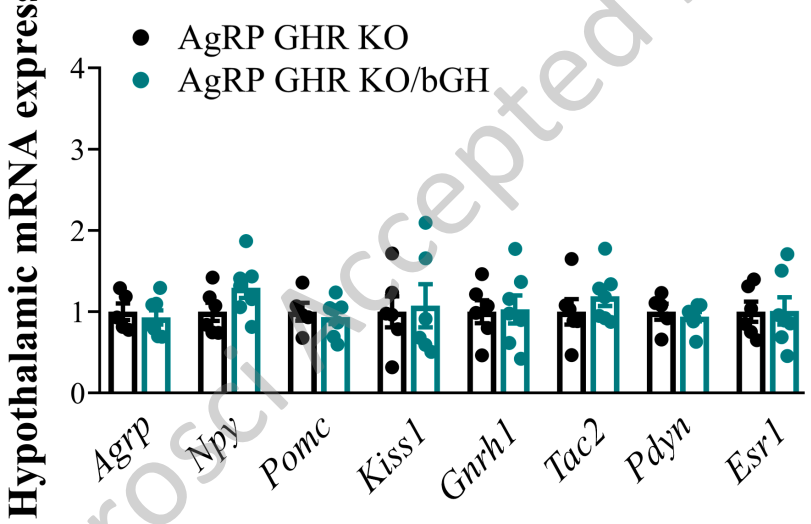


JNeurosci Accepted Manuscript

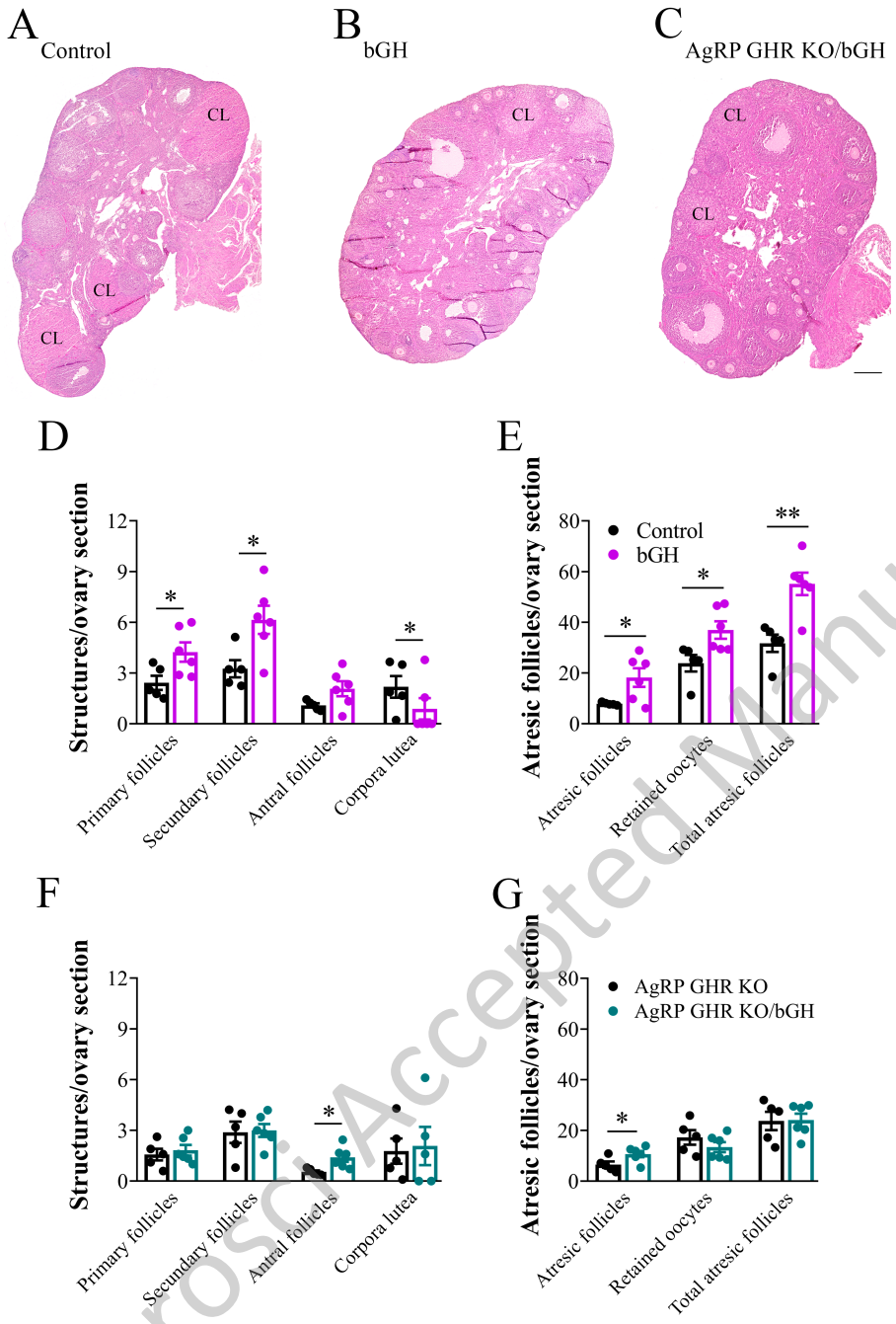
A



B



JNeurosci Accepted Manuscript



JNeurosci Accepted Manuscript